Desalination and Water Treatment
www.deswater.com

doi: 10.5004/dwt.2017.21366

89 (2017) 150–161
September

Application of response surface methodology for statistical analysis, modeling, and optimization of malachite green removal from aqueous solutions by manganese-modified pumice adsorbent

Amir Karami[a], Kamaleddin Karimyan[b,c], Reza Davoodi[a], Mostafa Karimaei[c,d], Kiomars Sharafie[e], Shoeib Rahimi[f], Touba Khosravi[a], Mohammad Miri[g,h], Hooshmand Sharafi[a], Ali Azari[a,*]

[a]*Research Center for Environmental Determinants of Health (RCEDH), Kermanshah University of Medical Sciences, Kermanshah, Iran, Tel.+989124528677; email: ali_azari67@yahoo.com (A. Azari), Tel. +989183598931; email: amir_karami119@yahoo.com (A. Karami), Tel. +989188592871; email: reza_yello_2000@yahoo.com (R. Davoodi), Tel. +989189318647; email: touba_khosravi@yahoo.com (T. Khosravi), Tel. +989186700327; email: hooshmand.sharafi@gmail.com (H. Sharafi)*
[b]*Environmental Health Research Center, Kurdistan University of Medical Sciences, Sanandaj, Iran, Tel. +989183787258; email: kamal.karimyan@gmail.com*
[c]*Department of Environmental Health Engineering, School of Public Health, Tehran University of Medical Sciences, Tehran, Iran*
[d]*Department of Environmental Health Engineering, Aradan School of Public Health and Paramedicine, Semnan University of Medical Sciences, Semnan, Iran, Tel. +989126605688; email: mostafakarimaee@gmail.com*
[e]*Department of Environmental Health Engineering, School of Public Health, Kermanshah University of Medical Sciences, Kermanshah, Iran, Tel. +989183786151; email:kio.sharafi@gmail.com*
[f]*Students Research Committee, Kermanshah University of Medical Sciences Kermanshah, Iran, Tel. +989189959772; email: shoeib94@yahoo.com*
[g]*Department of Environmental Health, School of Public Health, Sabzevar University of Medical Sciences, Sabzevar, Iran, Tel. +989189071725; email: m_miri87@yahoo.com*
[h]*Department of Environmental Health, School of Public Health, Shahid Sadoughi University of Medical Sciences, Yazd, Iran*

Received 17 February 2017; Accepted 22 August 2017

ABSTRACT

It is hard to remove malachite green from aquatic environments due to its low degradability and other features. Based on the effect of manganese on physical and chemical characteristics of scoria, the aim of this study is to evaluate the manganese–coated pumice performance in removing malachite green (MG) from aquatic environments. Response surface methodology (RSM) based on the central composite designs (CCD) was used to assess the effects of independent variables including pH (3, 5, 7, 9, and 11), adsorbent dosage (0.2, 0.5, 0.8, 1.1, and 1.4 g/L), contact time (15, 30, 45, 60, and 75 min), and constant concentration of the dye (85 mg/L) on the response function and the best response values were predicted. The results indicated that the dye removal increases with increasing the pH value, absorbent dosage and contact time, whereas MG concentration has an antagonistic effect on sorption system. Moreover, the optimum dye removal efficiency (99.9%) was achieved in pH = 11, adsorbent dose = 1.4 g/L, and contact time = 75 min. The adsorption process fitted well with the Langmuir model which, indicated the presence of heterogeneous sites for to adsorption MG dye and also this process followed the pseudo-second-order model. According to the results, the modified pumice with manganese could be successfully used for MG adsorption in the aqueous solution rather than natural scoria due to wide chemical changes of adsorbent structure.

Keywords: Adsorption; Malachite green dye; Manganese-coated pumice; Response surface methodology

* Corresponding author.

1944-3994/1944-3986 © 2017 Desalination Publications. All rights reserved.

1. Introduction

A huge pollution problem such as dye pollutants is produced from chemical industries (e.g., textile, leather, paper, and dye manufacturing industries) [1]. However, wide application of dyes are being produced in various processes of textile manufacture, which contributes to produce the colored wastewater flow which are extremely noxious to the aquatic biota and endanger the natural water resources balance through reducing the photosynthetic activity. Additionally, previous researches reported some adverse effects of dyes on human beings (e.g., allergy, dermatitis, skin irritation, and cancer) [2,3]. Textile effluent dyes create adverse effects on the surrounding environment due to their toxicity and slow decomposition. Therefore, removing dyes from wastewater effluents prior to mixing up with unpolluted natural water resources is significant [4]. Some common techniques such as coagulation, flocculation, oxidation, precipitation, filtration, electrochemical treatment, adsorption processes, etc., are launched to remove dyes from industrial wastewater [5–7]. The mentioned methods require chemical materials and large amounts of electrical energy which further poses problems to environment. It could be stated that removing dye from effluent by the mentioned chemical methods could create some troubles such as sludge accumulation and its disposal [8,9]. Among the above techniques, adsorption method seems to be the most effective method due to easy operation and handling. Adsorption is the most flexible process which was widely used for removing the pollutants from wastewaters [10,11]. The low cost, availability, microporous structure, and specific surface area of scoria powder make it an appropriate adsorbent material which can eliminate the preliminary step of the calcinations and the high-energy usage. In addition, it floats in water because of its low density. Recently, many researchers use scoria to remove cadmium, disinfection byproducts, heavy metals, phenol, various dyes, and sulfur dioxide from aqueous solutions [12,13]. Malachite green (MG) is an organic dye compound which is used as a dyestuff and – controversially – as an antimicrobial in aquaculture. Traditionally, malachite green was used as materials dye such as silk, leather, and paper [14–16]. Although this dye was not prepared from the mineral malachite, the name just comes from the similarity of color. Malachite green is classified in the dyestuff industry as a triarylmethane dye and is used in pigment industry [17]. Although the term malachite green is used loosely and often just refers to the colored cation, malachite green refers to the chloride salt $[C_6H_5C(C_6H_4N(CH_3)_2)_2]Cl$ formally. Also, the oxalate salt was marketed and the anions did not affect the color. The intense green color of the cation results from a strong absorption band at 621 nm (extinction coefficient of 10^5 $M^{-1}cm^{-1}$) [18]. Several studies were done in the field of removing malachite dye from aquatic environment so far. Ahmad and Alrozi [16] studied on adsorption of malachite green dye by date palm shell and found the absorption rate to be 19 mg/g and also indicated that by increasing pH the absorption rate was increased. Banerjee and Sharma [19] showed that the removal efficiency of malachite dye from waste wood was 93% in 100 min, adsorbent dose of 5 g/L, and initial dye concentration of 20 mg/L, and the adsorption process was in equilibrium. The aim of present study is statistical analysis, modeling, and optimization of malachite green removal from aqueous solutions by manganese-modified pumice adsorbent by application of response surface methodology (RSM).

2. Materials and methods

2.1. Chemicals and instruments

All chemicals used in this work were purchased from Merck Company (Germany). Natural pumice stones were collected from Tikmeh Dash Reign, East Azerbaijan province, Iran. MG (Merck) was used to prepare stock solution using deionized water. This was further diluted to the desired concentration for practical use. The pH of solutions was adjusted and controlled (Jenway, Model 3510) to desired values using either NaOH or HCl dilute solutions. Residual concentrations of dye were measured in 665 nm by a spectrophotometer (Cary 50, PerkinElmer Inc., US).

2.2. Preparation of adsorbents (raw pumice and Mn-modified pumice)

Pumice stone was sieved and particles were kept in 1% HCl for 24 h and washed several times with deionized water in order to remove the impurity of scoria stone. The particles were then dried in an oven at 105°C for 14 h. These fractions were coated with manganese (Mn) as follows: 50 g of scoria particles and 150 mL of 0.01 M Mn $(NO_3)_2$ solution were added to a beaker and pH was adjusted to 12 by adding 0.5 M NaOH solution. Thereafter, the beaker was placed on a shaker at laboratory temperature (25°C ± 1°C) for 72 h and then the obtained material was dried at 105°C in the oven for 24 h as well. In order to remove the traces of uncoated $Mn(NO_3)_2$ from the particles, the dried particles were washed again with double-distilled water and dried in the oven at 105°C for 24 h [20].

2.3. Characteristics of adsorbent

Several methods such as Fourier transform infrared spectroscopy (FTIR), X-ray diffraction (XRD) and scanning electron microscopy (SEM) were used to characterize the adsorbent. The structural analysis and functional groups of absorbent were analyzed with a Fourier transform infrared spectrometer (WQF-510) with a resolution of 4 cm^{-1} in the range of 400–4,000 cm^{-1} by KBr pellets technique. The surface morphology of synthesized adsorbent was analyzed using SEM (Philips XL30) technique. XRD (Shimadzu XRD-6000) was used to determine the chemical characteristics and composition of crystalline structures. The size and shape of samples were observed by transmission electron microscopy (TEM, PHILIPS, and EM 208 S 100 kV) at an accelerating voltage of 90 kV. Nitrogen adsorption–desorption analysis was used to study the specific surface area and pore structure of pumice and Mn-modified pumice samples (NOVA 2200 – Quantachrome Instruments, USA).

2.4. Batch studies

This experimental study was carried out in batch reactor and laboratory scale. The stock solution of MG was prepared by dissolving MG dye ($C_{23}H_{26}N_2CL$ and molecular weight of 364.5 g/mol) in deionized water. Operational concentration of MG solution (85 mg/L) was achieved by diluting the prepared stock solution in distilled water and was fixed in all experiments. 0.1 M HCl or 0.1 M NaOH solutions were used to adjust the pH. The uptake efficiency and maximum adsorption capacity of MG were calculated according to the following equations. In order to achieve better results, experiments were repeated three times and average values were exhibited as final results.

$$\text{Metal ions removal (\%)} = \frac{(C_0 - C_e)}{C_0} \times 100 \quad (1)$$

$$q_e = (C_0 - C_e)\frac{V}{M} \quad (2)$$

where R: uptake efficiency (%), C_0: the initial MG concentrations in the solution (mg/L), C_e: equilibrium MG concentrations after adsorption (mg/L), q_e: the adsorption capacity (mg g), V: the volume of solution, and m: Mn-modified pumice mass (g).

2.5. Design of experimental setup

The RSM based on central composite design (CCD) was used in order to determine the best conditions of experiments, to minimize the number of experiments, and to investigate the relationship between the measured responses (MG removal) and number of independent variables with the goal of optimizing the response (Design Expert 8.0, Stat-Ease Inc., Minneapolis, MN, USA). Three main independent parameters (initial pH (X1), contact time (min) (X2), and adsorbent dosage (g/L) (X3)) and the adsorption of MG dye by the Mn-modified pumice (response) were selected for the experimental design via CCD. In the CCD model, the number of experiments (N) was calculated with $N = 2^k + 2k + x_0$, where k is the number of parameters and x_0 is the number of central points. Therefore, the total number of runs was calculated to be 20 considering $k = 3$ and $x_0 = 6$. The actual values of variables (X_i) were coded as x_i by:

$$A_i = \frac{X_i - X_0}{\Delta x} \quad (3)$$

where A_i is the coded value of the variable, X_0 and Δx are the values of X_i at the center point and the step change, respectively. The experimental ranges and levels of the independent chosen variables are given in Table 1. The relationship between the input variables and response can be described by Eq. (4):

$$Y = b_0 + \sum_{i=1}^{n} b_i x_i + \sum_{i=1}^{n} b_{ii} x_i^2 + \sum_{i=1}^{n-1} \sum_{j=i+1}^{n} b_{ij} x_i x_j \quad (4)$$

where Y is the response (MG removal efficiency); b_0 is the constant response when all factors are set at the center point;

Table 1
Independent variables and their levels used in the experimental design

Variables	Symbols	Level (coded value)				
		$-\alpha(-1.5)$	–1	0	+1	$+\alpha(1.5)$
pH	A	3	5	7	9	11
Contact time, min	B	15	30	45	60	75
Adsorbent, g/L	C	0.2	0.5	0.8	1.1	1.4

b_i, b_{ii} and b_{ij} represent the linear coefficient, quadratic coefficient, and interaction coefficient, respectively; x_i is the coded value of the variables; and n is the number of independent variables. ANOVA statistics (R^2, adjusted R^2, F-test, and t-test), normal plots and residual analysis were used to analyze the results and to check the statistical significance of the fitted quadratic models. The significance of the regression coefficients was tested by F and Student's t-tests at a 95% confidence level.

2.6. Isotherm models study: non-linear regression

In the present study, in order to describe the adsorption processes at the equilibrium point the Langmuir, Freundlich, Temkin, and Dubinin–Radushkevich as two-parameter isotherm models and Sips, Redlich-Peterson, Toth and Khan as three-parameter isotherm models were fitted to the experimental data (Tables 2 and 3). The non-linear regression analysis was conducted using solver add-ins of Microsoft Excel® which minimizes the sum of the residual error to produce the best fitness of experimental data and to estimate the model coefficients. The selected optimum isotherm was goodness of fit (GooF) method. In GooF method, eight error functions (RMSE, χ^2, ERRSQ, HYBRID, MPSD, ARE, EABS, and APE) were selected and used to classify isotherms from the best to the worst. Different error functions may produce a different set of parameters for each isotherm. In this study, the best set of parameters for each isotherm was selected according to normalization/optimization method. In this method, the sum of normalized error (SNE) was calculated and used to select the best set of parameters.

3. Results and discussion

3.1. Characterization of adsorbent

The SEM images of the raw pumice surface and the Mn deposited on pumice showed that the surface of both sorbents is irregular and porous with large flakes (Figs. 1(a) and (b)). Mn-modified pumice sample shows that Mn (shine particle) is distributed non-asymmetrically on the surface of pumice. The SEM analysis also clarified the various size of Mn nanoparticles existing on surface of pumice.

The XRD patterns of raw and Mn-modified pumice are demonstrated in Fig. 2. Both adsorbents revealed similar peaks and this confirms that the modification process did not have a significant impact on the structural framework of the pumice. XRD patterns of natural and modified pumice can be determined by the peaks appeared at $2\theta = 12.0°$,

Table 2
Non-linear form of adsorption isotherm and kinetic models

Model	Equation	Equation	Equation	Reference
Two-parameter	Langmuir	$q_e = \frac{Q_0 K_L C_e}{1 + K_L C_e}$	(5)	[21]
	Freundlich	$q_e = K_F C_e^{1/n}$	(6)	[22]
	Temkin	$q_e = \frac{RT}{b_T} \ln A_T C_e$	(7)	[23]
	Dubinin–Radushkevich	$q_e = q_S \left[-BRT \ln(1 + \frac{1}{C_e}) \right]^2$	(8)	[24]
Three-parameter	Sips	$q_e = \frac{q_s K_s C_e^{m_s}}{1 + K_s C_e^{m_s}}$	(9)	[25]
	Redlich–Peterson	$q_e = \frac{K_R C_e}{1 + a_R C_e^{\beta}}$	(10)	[26]
	Toth	$q_e = \frac{K_T C_e}{(a_T + C_e)^{1/t}}$	(11)	[27]
	Khan	$q_e = \frac{q_s b_k C_e}{(1 + b_k C_e)^{a_k}}$	(12)	[28]

Note: K_L (L/mg), b_T (kJ/mol), K_F (mg/g), B (mol²/kJ²), Q_0: maximum monolayer coverage capacities (mg/g), n: adsorption intensity, A_T: equilibrium binding constant (L/g), q_s: theoretical isotherm saturation capacity (mg/g), R: gas constant (J/mol K), T: absolute temperature (K), C_e: equilibrium concentration (mg/L), and q_e: amount of adsorbate in the adsorbent at equilibrium (mg/g).

26.0°, 32.5°, 33.0°, 33.5°, 34.5°, and 28.0°. XRD dome-shaped curve between 2θ of 20° and 40° confirmed that both samples are amorphous by the halo-shaped diffusion band. It also shows that anorthite, calcite, quartz, and dolomite were available in the structure of raw and Mn-modified pumice [24].

The shape and size of Mn-modified pumice were examined using TEM micrographs at 100 KeV. Fig. 3 shows that the modified pumice contain flake and intertwined structure. TEM image (Fig. 3 inner) also confirmed that the Mn nanoparticles were well dispersed on the pumice surface. This analysis also indicated that the size of pumice is approximately between 50 and 84 nm and the Mn nanoparticles size is approximately 9 nm with deviation reliability of 95% (α = 5%).

Fig. 4 shows the FTIR analysis of the modified pumice before and after the adsorption of MG at wavelengths ranging from 400 to 4,000 cm^{-1}. The absorption bands at 1,043, 793, and 465 cm^{-1} can be allocated with symmetric stretching vibration of Si–O–Si (silica–oxygen compounds band). The broadening peaks at 3,519 and 1,640 cm^{-1} are related to the asymmetric stretching vibration of H–O bond and bending vibration of H–O–H bond, respectively. After MG adsorption, the new peak at 1,633 cm^{-1} was appeared which could be assigned to amide I or C=O amide stretching. The appearance of new peak at 1,633 cm^{-1} demonstrated that MG was adsorbed to the modified pumice with cation exchange and surface complexation [24].

The specific surface area, volume, and average pore diameter for manganese-coated pumice and raw pumice were measured using the BET method, and the results are given in Table 1. The results indicated that the surface area of the pumice and Mn-modified pumice were 41 and 49 m^2/g, respectively, indicating that the composite provides a higher adsorption capacity for pollutants compared with the raw pumice. As given in Table 4, the surface area, mean size, and pore volume of manganese-coated pumice were larger than the pumice before modification which can be due to the grafting of manganese (Mn) onto pumice. The average pore size of pumice before and after modification was estimated to be 2.9 and 3.4 nm, respectively. According to the IUPAC classification, the average sizes between 2 and 50 nm (2 nm < size < 50 nm) are classified into mesopore groups.

3.2. Regression models and statistical testing

The full factorial CCD with three factors in five levels, along with the maximum observed and predicted response are listed in Table 5. According to RSM results, the second-order polynomial equation was obtained for MG adsorption as shown in Eq. (21):

Table 3
Different error functions and equations

Error function	Abbreviation	Formula	Equation	Reference
Sum of squares errors	ERRSQ/SSE	$\sum_{i=1}^{n}(*q_{e,\text{calc}}-q_{e,\text{exp}})_i^2$	(13)	[23]
Hybrid fractional error function	HYBRID	$\frac{100}{n-p}\sum_{i=1}^{n}(\frac{q_{e,\text{exp}}-q_{e,\text{calc}}}{q_{e,\text{exp}}})_i$	(14)	[29]
Average relative error	ARE	$\frac{100}{n}\sum_{i=1}^{n}\left\lvert\frac{q_{e,\text{exp}}-q_{e,\text{calc}}}{q_{e,\text{exp}}}\right\rvert$	(15)	[30]
Sum of absolute error	EABS	$\sum_{i=1}^{n}\lvert q_{e,\text{exp}}-q_{e,\text{calc}}\rvert$	(16)	[29]
Marquardt's percent standard deviation	MPSD	$100\sqrt{\frac{1}{n-p}\sum_{i=1}^{n}(\frac{q_{e,\text{exp}}-q_{e,\text{calc}}}{q_{e,\text{exp}}})_i^2}$	(17)	[31]
Non-linear chi-square test	χ^2	$\sum_{i=1}^{n}\frac{\left(q_{e,\text{calc}}-q_{e,\text{exp}}\right)^2}{q_{e,\text{exp}}}$	(18)	[32]
Residual root mean square error	RMSE	$\sqrt{\frac{1}{n-2}\sum_{i=1}^{n}(q_{e,\text{exp}}-q_{e,\text{calc}})_i^2}$	(19)	[33]
Average percentage errors	APE	$\frac{\sum_{i=}^{n}\left\lvert\frac{q_{e,\text{exp}}-q_{e,\text{calc}}}{q_{e,\text{exp}}}\right\rvert_i}{p}\times 100$	(20)	[34]

Note: $q_{e,\text{calc}}$: calculated amount of adsorbate in the adsorbent at equilibrium (mg/g), $q_{e,\text{exp}}$: experimental amount of adsorbate in the adsorbent at equilibrium (mg/g), n: number of data point, and p: number of parameters within the isotherm equation.

$$Y\ (\text{MG adsorption}) = 64.13 + 32.18A + 3.32B + 6.06C - 1.91AB - 2.13AC - 0.33BC - 0.83A^2 - 2.83B^2 + 1.17\ C^2 \quad (21)$$

where A, B, and C represents pH, contact time, and adsorbent dosage, respectively. Eq. (21) reveals how parameters are affected by adsorption of MG dye by modified pumice. Negative and positive signs in Eq. (21) describe antagonistic and synergistic impacts of studied parameters on removal process. According to the obtained equations, all the parameters (A, B, and C) have positive effect on MG sorption confirming that the response (adsorption efficiency) was improved whenever the pH, contact time, and adsorbent dosage level increased. It could be approved that the maximum coefficient owned to A (pH) has the highest influence on MG dye adsorption process compared with the other ones.

3.3. Validity of the model

The significance of the data from MG adsorption was evaluated by ANOVA. Quadratic models along with multiple regression analysis were used to fit and calculate the results. The statistical analyses (variance analysis) of results for the response surface quadratic models are shown in Table 6. The values of determination coefficient, $R^2 > 0.99$, were obtained for MG dye removal and indicated that more than 99% of the total variability could be explained by the selected model (quadratic model) and only <1% of the total variations cannot be described via this model. In this study, the R^2-adj value was 0.9814, which proposed good correlations between the response and variables. The values of R^2-adj also proved the high significance of the quadratic model for MG adsorption process. On the other side, $p < 0.0001$ (p-value less than 0.05 revealed that the model terms are significant at confidence level of 95% or more) obtained for quadratic model in MG adsorption. This suggests that the model terms are significantly well in MG adsorption system. A low value of coefficient of variance of the model for MG dye removal was obtained to be 4.81% (<10%) indicating the precision and reliability of the experiments [35]. The lack-of-fit describes the variation of the data around the fitted model. In this study, the lack-of-fit > 0.05 obtained statistically insignificant for MG dye adsorption and showed a significant model correlation between the variables and MG dye removal. The model F-values of 112.24 and

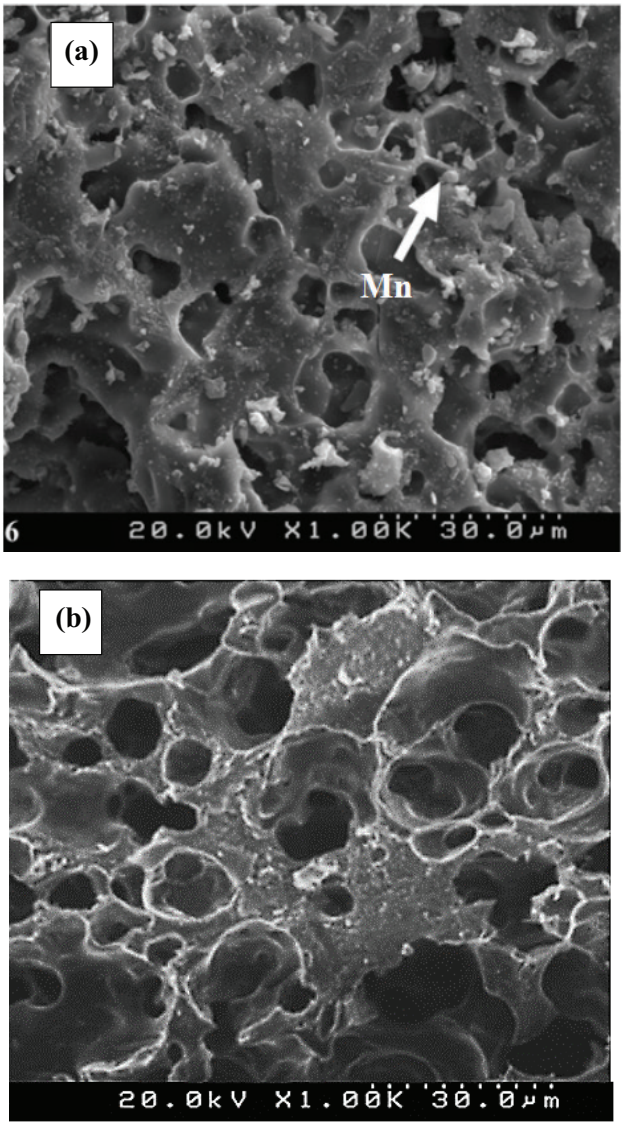

Fig. 1. Scanning electron microscopy (SEM) related to raw pumice (a) and Mn-modified pumice (b).

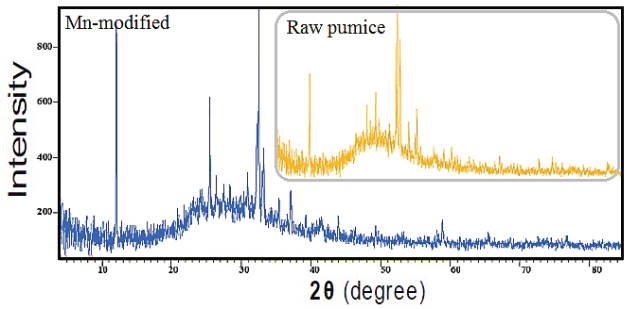

Fig. 2. XRD patterns of raw pumice (inner) and Mn-modified pumice.

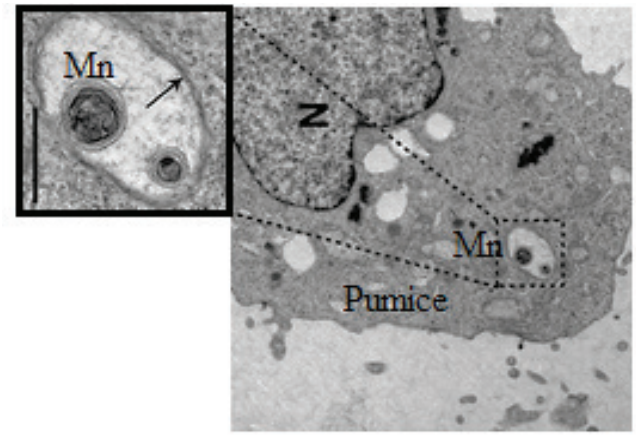

Fig. 3. TEM micrographs of synthesized Mn-modified pumice.

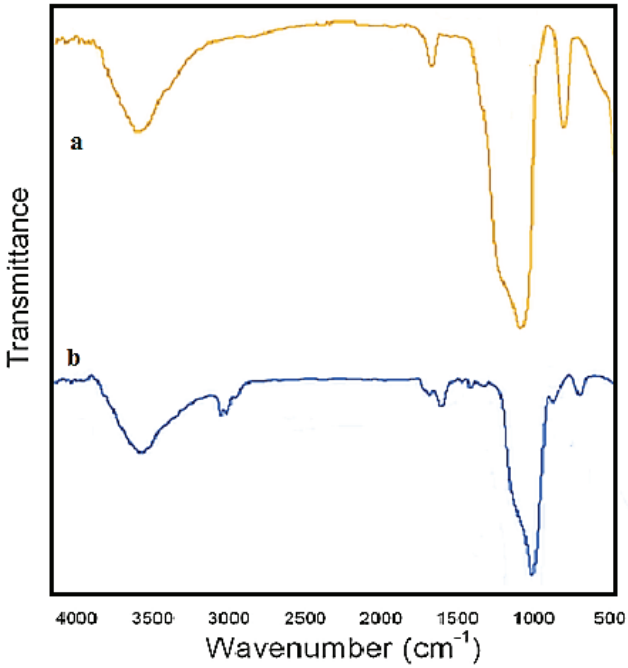

Fig. 4. Fourier transform infrared spectroscopy (FTIR) related to Mn-modified pumice before (a) and after MG adsorption (b).

Table 4
The BET specific surface areas, average pore size, and pore volumes of manganese-coated pumice and raw pumice

Sorbent	Pumice	Mn-modified pumice
Surface area (m^2/g)	41.96	49.34
Total pore volume (cm^3/g)	0.252	0.224
Average pore diameter (Ao)	2.9	3.4
Pore structure	Mesopore	Mesopore

adequate precision ratio > 38.23 indicate that the models for MG dye were significant and had adequate signals for the existing model. The ANOVA results also showed that the effect of all studied variables on response was significant ($p < 0.05$) and pH also affected the MG dye removal significantly.

Table 5
Response surface CCD design and results

STD	Variables			Responses (removal of dye, %)			
	Factor 1	Factor 2	Factor 3	Mn-modified pumice		Raw pumice	
	A: pH	*B*: contact time, min	*C*: adsorbent dosage, g/L	Actual	Predicted	Actual	Predicted
1	3	15	0.2	16	15.71	8	7.52
2	11	15	0.2	89.54	88.14	61.155	60.75
3	3	75	0.2	28	26.83	21	20.21
4	11	75	0.2	91.23	91.63	66.4225	66.72
5	3	15	1.4	33	32.74	21.75	21.61
6	11	15	1.4	95.34	96.65	69.505	70.45
7	3	75	1.4	41	42.54	29.75	30.31
8	11	75	1.4	98.4	98.82	71.8	72.44
9	5	45	0.8	48	47.84	32	33.07
10	9	45	0.8	82	80.01	60.5	56.91
11	7	30	0.8	61	61.76	44.75	44.28
12	7	60	0.8	68	65.09	50	47.95
13	7	45	0.5	57	61.40	41.75	43.89
14	7	45	1.1	74	67.45	53.5	48.84
15	7	45	0.8	62.8	63.33	45.1	45.02
16	7	45	0.8	63	64.03	43.25	44.11
17	7	45	0.8	62	61.16	44.5	45.41
18	7	45	0.8	63	65.13	46.25	46.23
19	7	45	0.8	64.1	64.13	44.075	46.01
20	7	45	0.8	64	64.14	46	46.51

The relationship between experimental and the predicted values for the MG dye adsorption on modified pumice are shown in Fig. 5. The good correlation between the data obtained by experiments and the predicted values by the model was observed ($R^2 > 0.934$). Fig. 5(b) shows normal probability plot of the studentised residuals for MG dye adsorption process. It could be found that the residual behavior follows a normal distribution and linear mode (Fig. 5(b)), which is a more essential supposition for checking the statistical modeling. In this research, the suggestion is to select a model for sufficient removal of MG dye using adsorption process [36,37].

3.4. Effect of variables on responses

Three dimensional (3D) response surface plots for evaluating the effects of three process parameters, that is, pH, contact time, and adsorbent dosage on efficiency of the adsorption process are depicted in Figs. 6 and 7. Fig. 6 represents the response surface plots of the initial pH and contact time on MG dye removal efficiency using Mn-coated pumice, while initial adsorbent dosage was fixed on 0.8 g/L. Fig. 6 shows that the removal efficiency of MG dye increases with increasing pH. A maximum dye removal was observed at pH = 11 and room temperature. As the adsorbent surface contains negative charge with increasing the pH, actually MG dye is a cationic dye and involves two nitrogen atoms that is a methyl factor [38]. Therefore, the negative charge of adsorbent surface increases in alkaline condition, resulting in the increasing dye adsorption due to the electrostatic attraction even in the pH more than 9 and the MG dye comprises more chemical changes so its adsorption increases too [39]. Also, the results showed that with decreasing the pH, the dye adsorption decreases and this could be due to the electrostatic repulsion in acidic condition because of producing the proton ions (H^+); therefore, the cationic dye adsorption will be reduced. Also, according to the point that the dominant pumice component is SiO_2, which is in term of decreasing the pH, its component changes to Si^{+3} which causes the electrostatic repulsion as a result of cationic dye adsorption reduction. Therefore, the poor dye adsorption in acidic condition is because of the dye penetration in adsorbent's pores [40]. Also, the high removal efficiency by the modified pumice in comparison with raw pumice in acidic pH takes place which could be due to the fact that although modifying pumice with manganese caused the increase in positive charge on the adsorbent surface, usually the cationic dye adsorption should be decreased due to the more electrostatic repulsion, but the high removal efficiency by the modified pumice occur in acidic pH in comparison with raw pumice despite the electrostatic repulsion is more. This confirmed that increasing the adsorbent efficiency by modifying pumice with manganese happens due to increase in the special surface of modified pumice in comparison with raw pumice [41]. Modifying pumice caused the irregular structure in pumice and this irregular structure increased the adsorption level [42]. Previous

Table 6
Analysis of variance (ANOVA) for response surface quadratic model

Source	Squares	df	Square	Value	Prob > F	
Model	9,301.4155	9	1,033.4906	112.24419	<0.0001	Significant
A-pH	8,800.9082	1	8,800.9082	955.83919	<0.0001	
B-contact time	93.889706	1	93.889706	10.197068	0.0096	
C-adsorbent dosage	311.66599	1	311.66599	33.849071	0.0002	
AB	29.070312	1	29.070312	3.157236	0.1060	
AC	36.252612	1	36.252612	3.9372832	0.0753	
BC	0.8646125	1	0.8646125	0.0939029	0.7656	
A^2	0.1299814	1	0.1299814	0.0141169	0.9078	
B^2	1.4994617	1	1.4994617	0.1628519	0.6950	
C^2	0.2534786	1	0.2534786	0.0275295	0.8715	
Residual	92.075198	10	9.2075198			
Lack-of-fit	88.960198	5	17.79204	28.558651	0.11	Non-significant
Pure error	3.115	5	0.623			
Cor. total	9,393.4907	19				
Std. dev.	3.0343895					
Mean	63.0705					
C.V. %	4.8111074					
Press	613.9567					
R-squared	0.990198					
Adj. R-squared	0.9813762					
Pred. R-squared	0.9346402					
Adeq. precision	38.735781					

studies also confirmed that studies by Kim et al. [43] and Vaughan and Reed [44] showed that the modified zeolite and activated carbon with aluminum and iron have more special surface in comparison with unmodified form of those metals.

The interactive effect of contact time and adsorbent dosage on removal efficiency in pH = 11 at 25°C is shown in Fig. 7. Dye removal efficiency increased rapidly with increasing contact time initially and attains a constant value later. It could be due to the adsorption sites occupied with adsorbate by increasing contact time and finally saturated adsorbent surface which is proved by Kakavandi et al. [45]. Fig. 7 showed that the maximum adsorption (95.6%) has been occurred at contact time 75 min and initial dosage of 1.4 g/L. Fig. 7 reveals that with increasing the adsorbent dosage from 0.2 to 1.4 g/L the removal efficiency increases. As shown in Fig. 7, the maximum uptake percentage for the MG dye was obtained at high adsorbent dosage (1.4 g/L) and contact time of 75 min. According to adsorbent dosage changes, the results showed that this change is more evident in comparison with contact time because with increasing doses, more adsorption sites would be available for adsorbent [46]. In fact, vacant active sites in initial time are the main reason of rapid sorption.

3.5. Adsorption isotherm

The results of isotherm ranking based on the value of the different error analysis are shown in table. The first rank is awarded to the isotherm with the least amount of the considered error function. As can be seen from Table 7, Temkin is the most visited isotherm in first ranking and next ranks belong to Freundlich and Langmuir, respectively.

As it can be seen from the table, for Langmuir isotherm, the modeled adsorption capacity (modeled q_e) curve obtained by minimizing the ARE error function had the most consistency with experimental adsorption capacity points (experimental q_e). The constants for Freundlich isotherm obtained by non-linear regression analysis are shown in Table 8. The best error function by which constants can be selected is APE. For Temkin isotherm, on the basis of SNE, MPSD is the best error function for modeling of data and obtaining the constants of the isotherm. Non-linear curve obtained by error analysis through applying different error functions were shown in Figs. 8–10 for Freundlich, Langmuir, and Temkin, respectively.

In order to evaluate the efficiency of the Mn-modified pumice in MG removal, a comparative study between applied sorbent in the present work and different adsorbents previously used for MG removal was done and the results

are given in Table 9. Based on the q_m obtained by Langmuir isotherm, it can be concluded that the synthesized adsorbent possesses a suitable sorption capacity, in comparison with the other sorbent's capacities. Differences of the adsorption capacities of the listed adsorbents can be due to the difference in their structure, surface area, and properties of functional groups in each adsorbent.

3.6. Mn leaching

In order to test whether Mn leach out into the solution from the Mn-modified pumice composite or not, the samples were analyzed by applying ICP-MS after each reaction cycle. Based on the results, the residuals of Mn were not detected under acidic, neutral, and basic conditions. It can be noticed that tendency of Mn leaching in the range of pH values is practically negligible (non-detected) and was less than recommended Mn standards for drinking water (0.05 mg/L). Considering the result of the present study, it can be speculated that Mn-modified pumice has acceptable stability and durability to strongly bind the metal to pumice, which can be regarded as an advantage for its recycling in continuous MG removal.

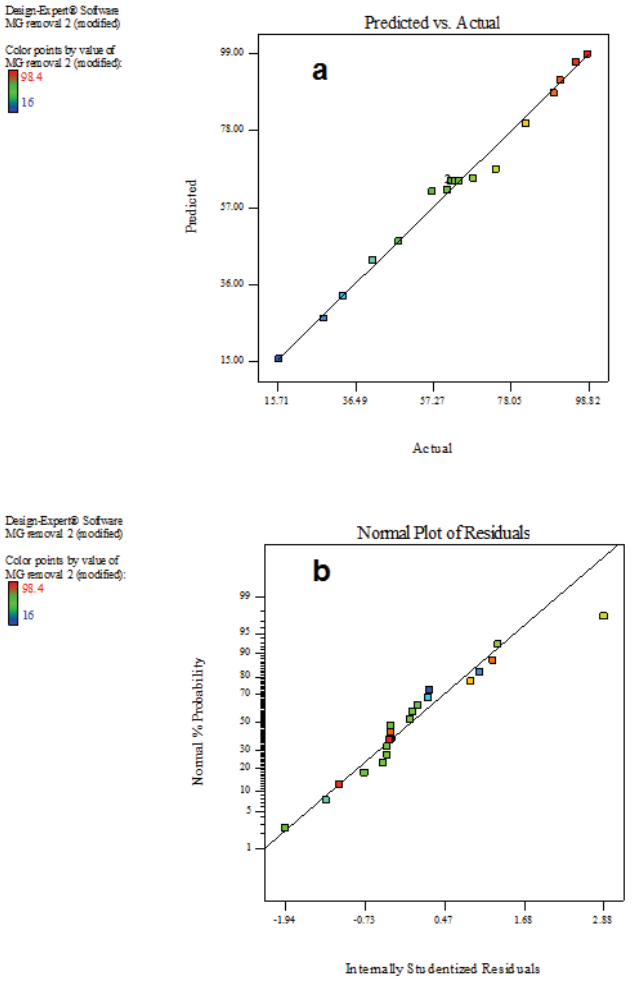

Fig. 5. Actual and predicted values of response for MG sorption (a) and normal probability plot of the studentised residuals for the selective dye adsorption process (b).

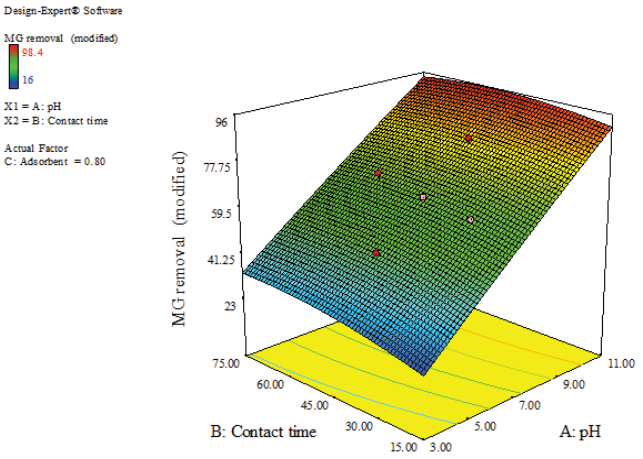

Fig. 6. Effect of contact time and pH on removal of MG dye by Mn-modified pumice (adsorbent dosage = 0.8).

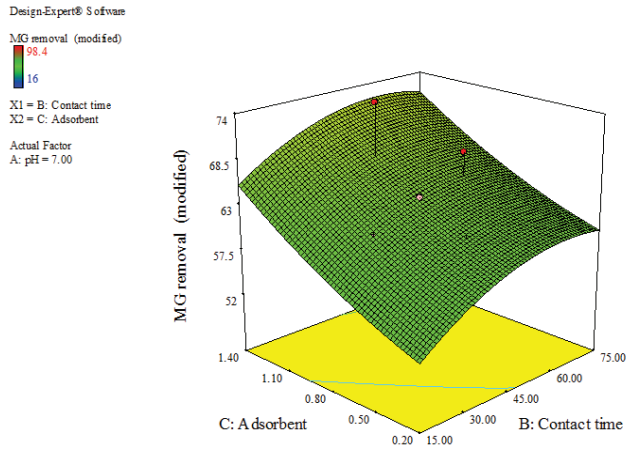

Fig. 7. Effect of contact time and adsorbent dosage on removal of MG dye by Mn-modified pumice (in pH = 11).

Table 7
Models ranking from the best to the worst based on GooF method

	RMSE	X2	ERRSQ	HYBRID	MPSD	APE	ARE	EABS	Most visited
Two-parameter	FR	TE	FR	TE	TE	TE	TE	TE	TE
	TE	FR	TE	FR	FR	FR	FR	FR	FR
	LA	LA	LA	LA	LA	LA	LA	LA	LA

Table 8
Constants of isotherm models obtained by minimizing different error functions

Isotherm	Parameter	RMSE	χ2	ERRSQ	Hybrid	MPSD	ARE	EABS	APE
Langmuir	Q_0	192.66	181.65	192.66	181.65	165.49	165.49	165.49	165.49
	b	0.53	0.71	0.53	0.71	1.02	0.84	0.84	0.84
	R_L	0.015	0.011	0.015	0.011	0.008	0.009	0.009	0.009
	R^2	0.956	0.963	0.956	0.920	0.923	0.923	0.923	0.963
Freundlich	K_F	68.12	61.76	68.12	61.76	57.34	52.40	52.40	52.40
	n	3.06	2.73	3.06	2.73	2.48	2.46	2.46	2.46
	R^2	0.982	0.975	0.982	0.975	0.955	0.946	0.946	0.946
Temkin	b_T	78.89	85.67	78.89	85.67	93.79	91.74	78.98	91.74
	A_T	13.18	17.14	13.18	17.14	20.11	20.82	11.71	20.82
	R^2	0.978	0.983	0.978	0.971	0.943	0.956	0.974	0.956

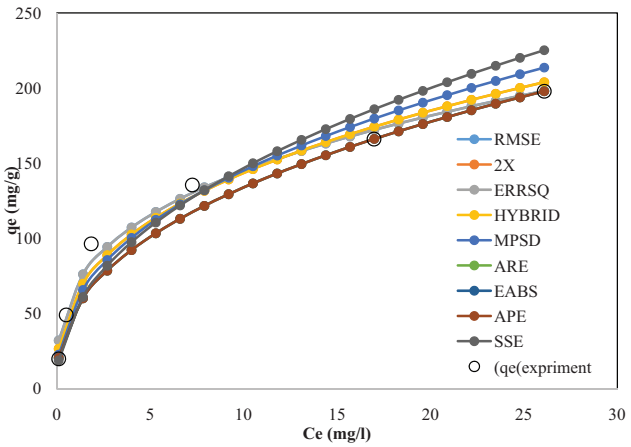

Fig. 8. Fitted non-linear curve to experimental data for Freundlich isotherm.

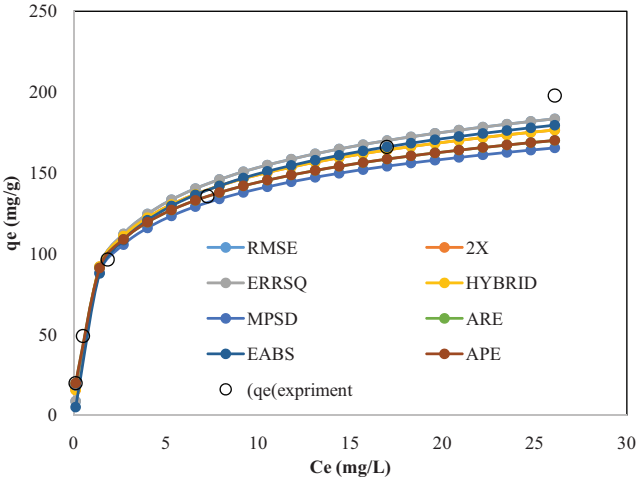

Fig. 10. Fitted non-linear curve to experimental data for Temkin isotherm.

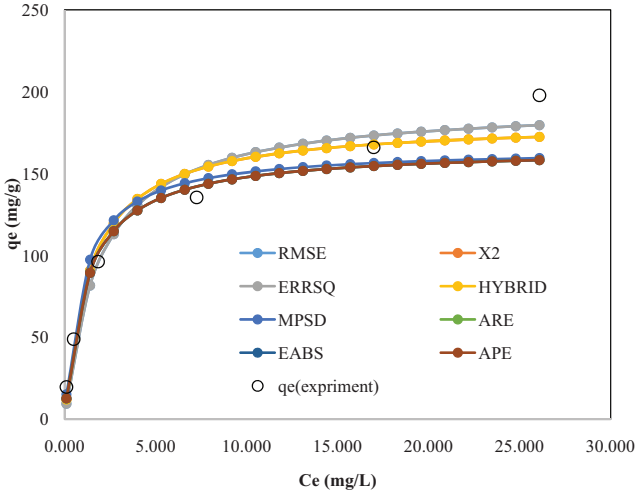

Fig. 9. Fitted non-linear curve to experimental data for Langmuir isotherm.

Table 9
Comparison of adsorption capacity of MG between various adsorbents found in the literatures

Adsorbent	q_m (mg/g)	Isotherms	Reference
Mn-modified pumice (25°C)	176.3	L	This work
Carboxylate-functionalized cellulose nanocrystals	243.9	L	[47]
Modified cellulose	131.93	L	[48]
Modified cellulose by anhydride	74	L	[49]
Activated carbon from corn cob (25°C)	52.63	L	[50]
Fe_3O_4@SiO_2–NH_2	156.32	F	[51]
Rambutan peel-based activated carbon	388	L	[16]

4. Conclusion

The results showed that removing of malachite green dye was increased by increasing pH, adsorbent dosage, and contact time. The highest efficiency (99.9%) obtained in pH = 11, adsorbent dose = 1.4 g/L, and contact time = 75 min. According to the results, it could be concluded that pumice modified with manganese increases the removal efficiency rather than raw scoria due to wide chemical changes of adsorbent structure.

Acknowledgment

The authors gratefully acknowledge the Research Council of Kermanshah University of Medical Sciences (Grant Number: 93049) for the financial support.

References

[1] E. Alkaya, G.N. Demirer, Sustainable textile production: a case study from a woven fabric manufacturing mill in Turkey, J. Clean. Prod., 65 (2014) 595–603.
[2] K. Sharafi, A.M. Mansouri, A.A. Zinatizadeh, M. Pirsaheb, Adsorptive removal of methylene blue from aqueous solutions by pumice powder: process modelling and kinetic evaluation, Environ. Eng. Manage. J., 14 (2015) 1067–1078.
[3] M.A. Zazouli, A. Azari, S. Dehghan, R.S. Malekkolae, Adsorption of methylene blue from aqueous solution onto activated carbons developed from eucalyptus bark and *Crataegus oxyacantha* core, Water Sci. Technol., 74 (2016) 2021–2035.
[4] F.B. Shahri, A. Niazi, Synthesis of modified maghemite nanoparticles and its application for removal of Acridine Orange from aqueous solutions by using Box-Behnken design, J. Magn. Magn. Mater., 396 (2015) 318–326.
[5] A. Ahmad, S.H. Mohd-Setapar, C.S. Chuong, A. Khatoon, W.A. Wani, R. Kumar, M. Rafatullah, Recent advances in new generation dye removal technologies: novel search for approaches to reprocess wastewater, RSC Adv., 5 (2015) 30801–30818.
[6] A. Azari, M. Gholami, Z. Torkshavand, A. Yari, E. Ahmadi, B. Kakavandi, Evaluation of Basic Violet 16 adsorption from aqueous solution by magnetic zero valent iron-activated carbon nanocomposite using response surface method: isotherm and kinetic studies, J. Mazandaran Univ. Med. Sci., 24 (2015) 333–347.
[7] R. Rezaei Kalantry, A. Jonidi Jafari, A. Esrafili, B. Kakavandi, A. Gholizadeh, A. Azari, Optimization and evaluation of reactive dye adsorption on magnetic composite of activated carbon and iron oxide, Desal. Wat. Treat., 57 (2016) 6411–6422.
[8] G.Z. Kyzas, D.N. Bikiaris, M. Kostoglou, N.K. Lazaridis, D.N. Bikiaris, Decolorization of Dyeing Wastewater Using Polymeric Absorbents – An Overview. In Eco-Friendly Textile Dyeing and Finishing, InTech, Rijeka, Croatia, 2013, pp. 177–205.
[9] A. Azari, R.R. Kalantary, G. Ghanizadeh, B. Kakavandi, M. Farzadkia, E. Ahmadi, Iron–silver oxide nanoadsorbent synthesized by co-precipitation process for fluoride removal from aqueous solution and its adsorption mechanism, RSC Adv., 5 (2015) 87377–87391.
[10] V.K. Gupta, R. Kumar, A. Nayak, T.A. Saleh, M. Barakat, Adsorptive removal of dyes from aqueous solution onto carbon nanotubes: a review, Adv. Colloid Interface Sci., 193 (2013) 24–34.
[11] A.J. Jafari, B. Kakavandi, R.R. Kalantary, H. Gharibi, A. Asadi, A. Azari, A.A. Babaei, A. Takdastan, Application of mesoporous magnetic carbon composite for reactive dyes removal: process optimization using response surface methodology, J. Korean Chem. Soc., 33 (2016) 2878–2890.
[12] M. Moradi, A.M. Mansouri, N. Azizi, J. Amini, K. Karimi, K. Sharafi, Adsorptive removal of phenol from aqueous solutions by copper (cu)-modified scoria powder: process modeling and kinetic evaluation, Desal. Wat. Treat, 57 (2016) 11820–11834.
[13] M. Moradi, L. Hemati, M. Pirsaheb, K. Sharafi, Removal of hexavalent chromium from aqueous solution by powdered scoria-equilibrium isotherms and kinetic studies. World Appl. Sci. J., 33 (2015) 393–400.
[14] D. Robati, M. Rajabi, O. Moradi, F. Najafi, I. Tyagi, S. Agarwal, V.K. Gupta, Kinetics and thermodynamics of malachite green dye adsorption from aqueous solutions on graphene oxide and reduced graphene oxide, J. Mol. Liq., 214 (2016) 259–263.
[15] H.I. Chieng, L.B. Lim, N. Priyantha, Enhancing adsorption capacity of toxic malachite green dye through chemically modified breadnut peel: equilibrium, thermodynamics, kinetics and regeneration studies, Environ. Technol., 36 (2015) 86–97.
[16] M.A. Ahmad, R. Alrozi, Removal of malachite green dye from aqueous solution using rambutan peel-based activated carbon: equilibrium, kinetic and thermodynamic studies, Chem. Eng. J., 171 (2011) 510–516.
[17] A. Gürses, M. Açıkyıldız, K. Güneş, M.S. Gürses, Classification of Dye and Pigments, in: Dyes and Pigments, Springer International Publishing, USA, 2016, pp. 31–45.
[18] Y. Song, S. Ding, S. Chen, H. Xu, Y. Mei, J. Ren, Removal of malachite green in aqueous solution by adsorption on sawdust, Korean J. Chem. Eng., 32 (2015) 2443–8.
[19] S. Banerjee, Y.C. Sharma, Equilibrium and kinetic studies for removal of malachite green from aqueous solution by a low cost activated carbon, Ind. Eng. Chem. Res., 19 (2013) 1099–1105.
[20] A. Salifu, B. Petrusevski, K. Ghebremichael, L. Modestus, R. Buamah, C. Aubry, G. Amy, Aluminum (hydr)oxide coated pumice for fluoride removal from drinking water: synthesis, equilibrium, kinetics and mechanism, Chem. Eng. J., 228 (2013) 63–74.
[21] A. Rahmani, M. Zarrabi, M. Samarghandi, A. Afkhami, H.R. Ghaffari, Degradation of Azo Dye Reactive Black 5 and acid orange 7 by Fenton-like mechanism, Iran. J. Chem. Eng., 7 (2010) 87–94.
[22] R. Shokoohi, M. Saghi, H. Ghafari, M. Hadi, Biosorption of iron from aqueous solution by dried biomass of activated sludge, Iran. J. Environ. Health Sci. Eng., 6 (2009) 107–114.
[23] G. McKay, A. Mesdaghinia, S. Nasseri, M. Hadi, M.S. Aminabad, Optimum isotherms of dyes sorption by activated carbon: fractional theoretical capacity & error analysis, Chem. Eng. J., 251 (2014) 236–247.
[24] M.N. Sepehr, A. Amrane, K.A. Karimaian, M. Zarrabi, H.R. Ghaffari, Potential of waste pumice and surface modified pumice for hexavalent chromium removal: characterization, equilibrium, thermodynamic and kinetic study, J. Taiwan Inst. Chem. Eng., 45 (2014) 635–647.
[25] B. Hameed, D. Mahmoud, A. Ahmad, Equilibrium modeling and kinetic studies on the adsorption of basic dye by a low-cost adsorbent: coconut (*Cocos nucifera*) bunch waste, J. Hazard. Mater., 158 (2008) 65–72.
[26] S. Chowdhury, P. Saha, Adsorption kinetic modeling of safranin onto rice husk biomatrix using pseudo-first-and pseudo-second-order kinetic models: comparison of linear and non-linear methods, Clean Soil Air Water, 39 (2011) 274–282.
[27] S. Yakout, E. Elsherif, Batch kinetics, isotherm and thermodynamic studies of adsorption of strontium from aqueous solutions onto low cost rice-straw based carbons, Carbon Sci. Technol., 1 (2010) 144–153.
[28] Y.-S. Ho, G. McKay, Kinetic models for the sorption of dye from aqueous solution by wood, Process Saf. Environ. Prot., 76 (1998) 183–191.
[29] K. Foo, B. Hameed, Insights into the modeling of adsorption isotherm systems, Chem. Eng. J., 156 (2010) 2–10.
[30] S. Shahmohammadi-Kalalagh, H. Babazadeh, Isotherms for the sorption of zinc and copper onto kaolinite: comparison of various error functions, Int. J. Environ. Sci. Technol., 11 (2014) 111–118.
[31] L. Chan, W. Cheung, S. Allen, G. McKay, Error analysis of adsorption isotherm models for acid dyes onto bamboo derived activated carbon, Chin. J. Chem. Eng., 20 (2012) 535–542.
[32] B. Subramanyam, A. Das, Linearized and non-linearized isotherm models comparative study on adsorption of aqueous phenol solution in soil, Int. J. Environ. Sci. Technol., 6 (2009) 633–640.

[33] M. Samarghandi, M. Hadi, S. Moayedi, F.B. Askari, Two-parameter isotherms of methyl orange sorption by pinecone derived activated carbon, Iran. J. Environ. Health Sci. Eng., 6 (2010) 285–294.
[34] M. Hadi, M.R. Samarghandi, G. McKay, Equilibrium two-parameter isotherms of acid dyes sorption by activated carbons: study of residual errors, Chem. Eng. J., 160 (2010) 408–416.
[35] A. Azari, B. Kakavandi, R.R. Kalantary, E. Ahmadi, M. Gholami, Z. Torkshavand, M. Azizi, Rapid and efficient magnetically removal of heavy metals by magnetite-activated carbon composite: a statistical design approach, J. Porous Mater., 22 (2015) 1083–1096.
[36] A. Azari, H. Gharibi, B. Kakavandi, G. Ghanizadeh, A. Javid, A.H. Mahvi, K. Sharafi, T. Khosravia, Magnetic adsorption separation process: an alternative method of mercury extracting from aqueous solution using modified chitosan coated Fe_3O_4 nanocomposites, J. Chem. Technol. Biotechnol., 92 (2017) 188–200.
[37] S. Coruh, S. Elevli, Optimization of malachite green dye removal by sepiolite clay using a central composite design, Global Nest J., 16 (2014) 339–347.
[38] R. Ahmad, R. Kumar, Adsorption studies of hazardous malachite green onto treated ginger waste, J. Environ. Manage., 91 (2010) 1032–1038.
[39] A. Azari, A.H. Mahvi, S. Naseri, K.R. Rezaei, M. Saberi, Nitrate removal from aqueous solution by using modified clinoptilolite zeolite, Arch. Hyg. Sci., 3 (2014) 184–192.
[40] C.W. Muriuki, Evaluation of Banana Peels, Pumice and Charcoal Potential to Adsorb Chromium Ions from Tannery Wastewater, The Thesis of Masters Degree for Environmental Engineering and Management in Jomo Kenyatta University of Agriculture and Technology, 2016.
[41] M. Heidari, F. Moattar, S. Naseri, M. Samadi, N. Khorasani, Evaluation of aluminum-coated pumice as a potential arsenic (V) adsorbent from water resources, Int. J. Environ. Res., 5 (2011) 447–456.
[42] M.R. Samarghandi, M. Zarrabi, A. Amrane, G.H. Safari, S. Bashiri, Application of acidic treated pumice as an adsorbent for the removal of azo dye from aqueous solutions: kinetic, equilibrium and thermodynamic studies, Iran. J. Environ. Health Sci. Eng., 9 (2012) 9.
[43] Y. Kim, C. Kim, I. Choi, S. Rengaraj, J. Yi, Arsenic removal using mesoporous alumina prepared via a templating method, Environ. Sci. Technol., 38 (2004) 924–931.
[44] R.L. Vaughan, B.E. Reed, Modeling As (V) removal by a iron oxide impregnated activated carbon using the surface complexation approach, Water Res., 39 (2005) 1005–1014.
[45] B. Kakavandi, A. Jonidi Jafari, R. Rezaei Kalantary, S. Nasseri, A. Esrafili, A. Gholizadeh, A. Azari, Simultaneous adsorption of lead and aniline onto magnetically recoverable carbon: optimization, modeling and mechanism, J. Chem. Technol. Biotechnol., 91 (2016) 3000–3010.
[46] B. Hameed, M. El-Khaiary, Malachite green adsorption by rattan sawdust: isotherm, kinetic and mechanism modeling, J. Hazard. Mater., 159 (2008) 574–579.
[47] H. Qiao, Y. Zhou, F. Yu, E. Wang, Y. Min, Q. Huang, L. Pang, T. Ma, Effective removal of cationic dyes using carboxylate-functionalized cellulose nanocrystals, Chemosphere, 141 (2015) 297–303.
[48] Y. Zhou, X. Wang, M. Zhang, Q. Jin, B. Gao, T. Ma, Removal of Pb (II) and malachite green from aqueous solution by modified cellulose, Cellulose, 21 (2014) 2797–2809.
[49] Y. Zhou, Y. Min, H. Qiao, Q. Huang, E. Wang, T. Ma, Improved removal of malachite green from aqueous solution using chemically modified cellulose by anhydride, Int. J. Biol. Macromol., 74 (2015) 271–277.
[50] M.A. Palukurty, T. Allu, A. Chitturi, S.R. Somalanka, Adsorption of malachite green from synthetic waste water onto activated carbon from corn cob, J. Chem. Biol. Phys. Sci., 4 (2014) 1910.
[51] L. Sun, S. Hu, H. Sun, H. Guo, H. Zhu, M. Liu, H. Sun, Malachite green adsorption onto Fe_3O_4@ SiO_2-NH_2: isotherms, kinetic and process optimization, RSC Adv., 5 (2015) 11837–11844.